Editors' Suggestion

Topological Transport of Deconfined Hedgehogs in Magnets

Ji Zou◉, Shu Zhang,[*] and Yaroslav Tserkovnyak

Department of Physics and Astronomy, University of California, Los Angeles, California 90095, USA

We theoretically investigate the dynamics of magnetic hedgehogs, which are three-dimensional topological spin textures that exist in common magnets, focusing on their transport properties and connections to spintronics. We show that fictitious magnetic monopoles carried by hedgehog textures obey a topological conservation law, based on which a hydrodynamic theory is developed. We propose a nonlocal transport measurement in the disordered phase, where the conservation of the hedgehog flow results in a nonlocal signal decaying inversely proportional to the distance. The bulk-edge correspondence between the hedgehog number and skyrmion number, the fictitious electric charges arising from magnetic dynamics, and the analogy between bound states of hedgehogs in ordered phase and the quark confinement in quantum chromodynamics are also discussed. Our study points to a practical potential in utilizing hedgehog flows for long-range neutral signal propagation or manipulation of skyrmion textures in three-dimensional magnetic materials.

Introduction.—A main theme of spintronics is the utilization of spin degrees of freedom for information transmission and processing [1,2], either using spin-polarized electric currents, or relying on spins alone to free the transport from Joule heating. Magnons, the quanta of spin waves, have been proposed to be promising data carriers in new computing technologies [3–7]. A detectable diffusive spin transport can be achieved via magnons in ordered magnetic insulators [8] or even spin-conserving fluctuations in paramagnets [9]. However, such spin currents typically decay exponentially, once the propagation distance exceeds the spin-relaxation length [2]. In alternative transport regimes, where signals are expected to decay algebraically, topology plays a crucial role [10–12]. Topological spin textures, such as chiral domain walls [13], vortices [14–17], skyrmions [18–20], hopfions [21,22], and hedgehogs [23–26] are defined homotopically and are topologically protected [10–12]. Consequently, they are promising to sustain long-distance transport, even in the absence of local spin conservation.

While extensive studies have been devoted to spin textures in low dimensions, three-dimensional (3D) textures such as hedgehogs and hopfions are recently attracting more attention for their rich physics in topological phases [23–26] and dynamic properties [21,22,27,28]. Hedgehogs exist inherently in 3D Heisenberg magnets. In contrast to 3D skyrmions [29] and hopfions [21,22], which can be annihilated by shrinking them down to the size of the atomic spacing without affecting spins far away, hedgehogs cannot be removed via local surgeries. The hedgehog flow can therefore be more stable against thermal fluctuations, and has potential applications in memory, logic devices, and energy storage [30–35].

In this Letter, we explore both topological and energetic properties of magnetic hedgehogs in 3D Heisenberg ferromagnets to investigate their long-distance transport, the viability of which is considered from the following three aspects. A topological conservation law, which is valid in both the magnetically ordered and disordered phase, defines the framework of a hydrodynamic description of hedgehog currents. While (anti)hedgehogs are bound by a linear potential energy in the magnetically ordered phase, they become deconfined and hence mobile in the paramagnetic phase. We propose a nonlocal transport measurement in the setup as shown in Fig. 1. A conserved hedgehog flow can be driven by a transverse electric current applied at an adjacent metal contact, resulting in a nonlocal signal decaying inversely proportional to the system length in the flow direction.

Topological conservation law.—Let us first consider a 3D insulating ferromagnet without accounting for its detailed energetics, but focusing on topological aspects of its vectorial order parameter $\mathbf{n}(\vec{r}, t)$, where the bold face is used for axial vectors and the vector arrow marks polar vectors. In the ordered phase, the collinear magnetic order can be described by the directions of $\mathbf{n}$ assuming $|\mathbf{n}| = 1$. This would render a sphere order-parameter space S^2, with a nontrivial second homotopy group $\pi_2(S^2) = \mathbb{Z}$ [36]. A point defect, named hedgehog, with an integer-valued topological charge can correspondingly be identified in $\mathbf{n}(\vec{r}, t)$. A familiar example for a hedgehog placed at the origin is $\mathbf{n}_0 = \{x, y, z\}/|\vec{r}|$.

In the paramagnetic phase, the corresponding (coarse-grained) vector field $\mathbf{n}(\vec{r}, t) \in \mathbb{R}^3$ realizes an $\mathbb{R}^3 \to \mathbb{R}^3$ mapping at any given time t. This field texture is devoid of
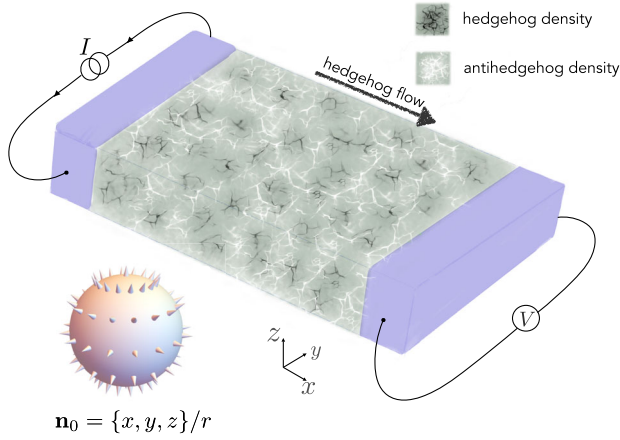
FIG. 1. A schematic for nonlocal transport measurement of hedgehog currents in a three-dimensional insulating magnet. Two metallic contacts are bridged by a magnetic insulator with hedgehog excitations. In the paramagnetic phase, hedgehogs are free to diffuse, where black and white ripples stand, respectively, for delocalized hedgehog and antihedgehog densities. An applied electric current I along y within the left metal transfers spin flow into the magnetic texture, which biases a hedgehog flow along x. Reciprocally, the hedgehog flow reaching the right terminal builds up a detectable electric voltage V. The nonlocal drag resistivity, $\varrho \propto V/I$, quantifies the efficiency of the topological hedgehog transport as well as their interfacial exchange coupling with conducting electrons. We also show a familiar example of a hedgehog $\mathbf{n}_0 = \{x, y, z\}/r$.

defects characterized by the aforementioned quantized charges, since the homotopy group $\pi_2(\mathbb{R}^3)$ is trivial [36]. Nevertheless, the smooth field $\mathbf{n}(\vec{r}, t)$ exhibits a topological hydrodynamics governed by the *topological conservation law* $\partial_\mu j^\mu = 0$ (with the Einstein summation implied over the Greek indices: $\mu = 0, 1, 2, 3 \leftrightarrow t, x, y, z$), where

$$j^\mu = \epsilon^{\mu\nu\alpha\beta} \partial_\nu \mathbf{n} \cdot (\partial_\alpha \mathbf{n} \times \partial_\beta \mathbf{n})/8\pi. \tag{1}$$

Here, $\epsilon^{\mu\nu\alpha\beta}$ is the Levi-Civita symbol with convention $\epsilon^{0123} = 1$. The conserved (topological) charge within a bulk Ω is

$$\mathcal{Q} \equiv \int_\Omega dx\,dy\,dz\, j^0 = \frac{1}{8\pi} \int_{\partial\Omega} dx^j \wedge dx^k \mathbf{n} \cdot (\partial_j \mathbf{n} \times \partial_k \mathbf{n}), \tag{2}$$

which equals the skyrmion number at boundary $\partial\Omega$, according to the generalized Stokes' theorem [36]. We recognize that charge $\mathcal{Q}$ is precisely the hedgehog number (thus j^μ is the hedgehog current) in the ordered phase, with the last equality in Eq. (2) defining the degree of the $S^2 \to S^2$ mapping on the boundary. Our simple example $\mathbf{n}_0$ yields $j^0 \to \delta(\vec{r})$ and thus $\mathcal{Q} = 1$. Here, we remark that the core should be regularized. There is no true singularity in our treatment. In the paramagnetic phase, $\mathcal{Q}$ is no longer

quantized due to fluctuations in the magnitude of $\mathbf{n}$. Regardless, the hedgehog current, Eq. (1), is conserved [37], which sets the stage for the topological hydrodynamics of hedgehogs at an arbitrary temperature. The conservation law also holds in the lattice limit, with proper discretized definitions [37]. Hereafter, we refer to $j^\mu = (j^0, \mathbf{j})$ as hedgehog density (and flux), irrespective of the temperature.

We stress that, in contrast to two-dimensional skyrmions [18–20] or three-dimensional Shankar skyrmions [29], which can be created and annihilated locally, the conservation law of hedgehogs is immune to local fluctuations and therefore applicable also in the paramagnetic phase [37]. This robustness of hedgehog flow underpins the hedgehog hydrodynamics.

Equation (2) establishes a bulk-edge correspondence, indicating that the total hedgehog number in a bulk interior can fluctuate only by flowing in and out through its boundary. This, in turn, is associated with a corresponding change in the skyrmion number on the boundary, acting as a fingerprint of the hedgehog flow. A close analog in lower dimensions has been thoroughly studied in the context of superfluid phase slips, where the winding number associated with one-dimensional *XY* textures can be changed by a transverse passage of planar vortices. The 3D bulk-edge correspondence Eq. (2) manifests when a skyrmion density unwinds or reversely builds up as a thread of a hedgehog current passes through, which has been verified experimentally [41].

Topological Maxwell equations.—We provide, in this section, another formulation of the conservation law as topological Maxwell equations, making connections to the well-known emergent electromagnetic fields associated with generic spin textures [42–48]. The divergence-free condition $\partial_\mu j^\mu = 0$ can be automatically satisfied by defining the current j^μ as a curl of a rank-2 antisymmetric Maxwell field-strength tensor

$$\mathcal{F}_{\alpha\beta} \equiv \mathbf{n} \cdot (\partial_\alpha \mathbf{n} \times \partial_\beta \mathbf{n})/4\pi, \tag{3}$$

whose components are the familiar electromagnetic fields:

$$E^i = \mathbf{n} \cdot (\partial_t \mathbf{n} \times \partial_i \mathbf{n})/4\pi, \quad \epsilon_{ijk} B^k = \mathbf{n} \cdot (\partial_i \mathbf{n} \times \partial_j \mathbf{n})/4\pi. \tag{4}$$

The hedgehog current Eq. (1) can therefore be recast into the form of the Maxwell equations:

$$\epsilon^{\mu\nu\alpha\beta} \partial_\nu \mathcal{F}_{\alpha\beta}/2 = j^\mu, \qquad \partial_\mu \mathcal{F}^{\mu\nu} = j_e^\nu. \tag{5}$$

The second equation defines the electric four-current, which is also conserved: $\partial_\mu j_e^\mu = 0$, following from the antisymmetric property of $\mathcal{F}$.

Note that fictitious electric and magnetic charges (as sources for $\vec{E}$ and $\mathbf{B}$) have the same symmetries as the real

electric and magnetic charges under both time-reversal and parity operations. The magnetic hedgehog with a quantized topological charge can be identified as a Dirac monopole. In the ordered phase, the quantization can also be understood from the view of the U(1) gauge structure of magnons. For a Heisenberg magnet, one may regard a fixed spin texture $\mathbf{n}(\vec{r})$ to spontaneously break the SU(2) symmetry of the spin algebra. The excitations thus have a smooth part, which can be viewed as describing regular spin waves, and a (singular) topological part, such as hedgehogs in our case. Therefore, the magnetic charges are quantized on a U(1) kernel [42,45,49], reminiscent of the 't Hooft and Polyakov approaches to the non-Abelian Higgs model [50]. For the (fictitious) electric sector, both the electric field and the electric charge density emerge solely out of the dynamics of the field configuration. According to the Gauss law, the total electric charge associated with a general local dynamics vanishes (see Supplemental Material [37] for electric charge distributions resulted from global dynamics). We restrict our discussion hereafter to the magnetic part.

Confinement and deconfinement.—We now turn to the energetics and physical dynamics of hedgehogs in Heisenberg magnets. Hedgehogs are confined in the ordered phase, with the potential energy of a hedgehog-antihedgehog pair growing linearly with their separation [51]. One can imagine a string of tension $4\pi\mathcal{A}$ tying them, where $\mathcal{A}$ is the exchange stiffness of the magnetic material [see Eq. (6) below]. The confinement is also expected from evaluating the potential energy of a single hedgehog,

$$\mathcal{U} = 4\pi\mathcal{A}R, \qquad (6)$$

where R is the size of the system. One can directly check this for $\mathbf{n} = \mathbf{n}_0$ placed at the origin of a sphere of radius R. For a hedgehog-antihedgehog pair, all flux from the hedgehog must end at the antihedgehog, forming a flux tube to minimize the energy. Such a system could realize an experimentally accessible analogy to quark confinement in QCD [52,53].

In the paramagnetic phase, hedgehogs deconfine naturally due to the absence of long-range correlations. Conceptually, the transition to the magnetically disordered phase can be thought of as a result of proliferation of hedgehogs, which form a two-component hedgehog-antihedgehog plasma (while topological charges are no longer quantized) as illustrated in Figs. 1 and 2. This extends our analogy with the QCD picture: Quarks deconfine and form a so-called quark-gluon plasma at high temperatures where the chiral symmetry is restored and long-range correlation is melted away [54–57]. The hedgehog system is therefore a promising alternate to study QCD theories in condensed matter systems. Previously considered was the magnetic monopole confinement in superconductors due to the Meissner effect [58–62], where
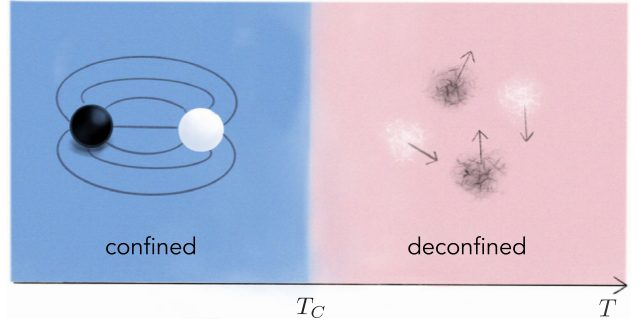

FIG. 2. Different phases of hedgehogs. At temperatures above the Curie temperature T_C, hedgehogs (black ripples) and anti-hedgehogs (white ripples) carrying nonquantized topological charges proliferate and become mobile. In the ordered phase, hedgehogs are confined by a linear potential analogous to the quark confinement in QCD. They are singular quantized objects, represented by black and white spheres.

monopoles enter a deconfined phase as the temperature increases, accompanying the superconductor-insulator transition.

We remark that hedgehogs are not always energy-costly excitations as in Heisenberg magnets. $MnSi_{1-x}Ge_x$ has a stable phase of a hedgehog-antihedgehog lattice [23–25], where there is evidence that four- and six-spin interactions may play an important role [63–65]. Here, we formally adopt a nonlocal term, which is particularly compatible with our fictitious electromagnetic formalism, into our Heisenberg Hamiltonian:

$$\mathcal{U} = \int d^3\vec{r}\left[\frac{\mathcal{A}}{2}(\vec{\nabla}\mathbf{n})^2 + \frac{\mathcal{C}}{2}(\partial_i\mathbf{n} \times \partial_j\mathbf{n})^2\right], \qquad (7)$$

where Einstein summation is implied over the i, j and $\mathcal{C}$ is a phenomenological parameter. Other quartic terms, such as $(\vec{\nabla}\mathbf{n})^4$, are also present in principle, but the above $\mathcal{C}$ term is of special interest to us. It resembles the Maxwell magnetic field energy $\propto \mathbf{B}^2$ (in the ordered phase, s.t. $|\mathbf{n}| \approx 1$). The total potential energy for a hedgehog is thus $\mathcal{U} \sim \mathcal{A}R - \mathcal{C}/R$, which indicates that hedgehogs are free at a small distance $r \ll \sqrt{\mathcal{C}/\mathcal{A}}$, where the Coulombic term dominates. This phenomena mimics the asymptotic freedom in QCD [52,53]. Likewise, in a system of small size, the hedgehog confinement becomes insignificant when $\sqrt{\mathcal{C}/\mathcal{A}}$ is comparable to R.

Biased hedgehog flow.—At the heart of the hedgehog transport is the (desired) capability of driving and manipulating the hedgehog current. We focus on the dynamics near the Curie temperature of a ferromagnet, where the hedgehogs get deconfined, while the thermal fluctuations are still not too violent atomistically. The spin dynamics can be described by $\partial_t\mathbf{n} = -\Gamma\mathbf{H}$, where we allow the magnitude $|\mathbf{n}|$ to fluctuate. $\mathbf{H} = \delta F/\delta\mathbf{n}$ is the effective field (with F being the free energy of the ferromagnet) and Γ is a

phenomenological dissipative coefficient. As illustrated in Fig. 1, we apply a linear electric current density (i.e., current per z thickness) $\vec{\mathcal{J}} = \mathcal{J}\hat{y}$ in the left metal contact. Given that the mirror-reflection symmetry is broken along the z axis, symmetry considerations [20,29,66,67] suggest that a spin flow can be transferred (per unit area) into the magnetic texture, in the form

$$\mathfrak{I} = \frac{3\hbar}{8e\pi}(\vec{\zeta} \cdot \vec{\nabla}\mathbf{n}) \times (\vec{\mathcal{J}} \cdot \vec{\nabla}\mathbf{n}), \qquad (8)$$

where $\vec{\zeta} = \zeta\hat{z}$ is a phenomenologically constructed vector (with the dimension of length), which reflects the mirror-symmetry breaking in the z direction. Note that the spin transfer $\mathfrak{I}$ is isotropic in spin space and thus does not rely microscopically on the presence of a spin-orbit coupling. We also remark that $\mathfrak{I}$ is constructed phenomenologically based on symmetry considerations. Its microscopic origin, magnitude, and direct experimental signatures remain to be explored.

In the presence of this spin transfer, we have $\partial_t\mathbf{n} = -\Gamma\mathbf{H} + \mathfrak{I}/s$, where s is the saturated spin density. The rate of change of the free energy density is thus $P = \partial_t\mathbf{n} \cdot \mathbf{H} = \mathfrak{I} \cdot \partial_t\mathbf{n}/s\Gamma - (\partial_t\mathbf{n})^2/\Gamma$. Here, the second term is the Rayleigh dissipation and the first term yields the total work done by the left contact upon magnetic dynamics:

$$W = \int dydzdt \frac{\mathfrak{I} \cdot \partial_t\mathbf{n}}{s\Gamma} = \frac{\hbar\zeta\mathcal{J}}{2es\Gamma}\mathcal{Q}. \qquad (9)$$

Note the work is proportional to the topological charge $\mathcal{Q}$. The setup in Fig. 1 therefore discriminates between topological charges of opposite signs, biasing a net hedgehog current. We also remark that mirror symmetry in the z direction is the minimal symmetry we need to break, in order for $\vec{\zeta}$ to effectively realize a polar vector in Eq. (8). As a symmetry-allowed process, a hedgehog current can be generated naturally as a channel to release the energy associated with electron dynamics in the left contact (where an electric current is applied, see Fig. 1). The electric current in the (left) metal contact provides an effective boundary bias for the hedgehog flow into the bulk, effectively establishing a local chemical potential for hedgehogs:

$$\bar{\mu}_L \equiv \frac{\delta W}{\delta\mathcal{Q}} = \frac{\hbar\zeta\mathcal{J}}{2es\Gamma}. \qquad (10)$$

Nonlocal spin drag.—We are now ready to study the transport of hedgehogs in the geometry depicted in Fig. 1. To this end, we operate the system in the paramagnetic phase, such that hedgehogs become mobile, rendering a finite effective hedgehog conductivity σ. We employ an Ohmic constitutive relation $j_x = -\sigma\partial_x\mu$ within the magnet. At the left boundary, using an electric current, the chemical

potential for hedgehogs is raised by $\bar{\mu}_L$. At the right terminal, which serves as the ground, the natural chemical potential vanishes, as hedgehogs can freely go in and out through the right boundary. The hedgehog flow in the y and z directions is nonvanishing in general [37]. Here we assume translational invariance along these two directions and focus on dynamics in the x direction. By invoking the reaction-rate theory [68], we obtain the hedgehog inflow and outflow at the left and right boundaries:

$$j_x^L = 2\gamma_L(\bar{\mu}_L - \mu_L)/k_BT, \qquad j_x^R = 2\gamma_R\mu_R/k_BT, \quad (11)$$

in linear response. Here, $\mu_{L,R} \equiv \mu(x = 0, L)$ is the chemical potential at two ends of the magnet, where L is its length along the x direction. $\gamma_{L,R} \sim \nu_{L,R}e^{-E_0/k_BT}$ is the equilibrium injection rate of hedgehogs at the respective boundaries, in terms of the attempt frequencies $\nu_{L,R}$ and an effective energy barrier E_0 governed by the core energy. Continuity of the hedgehog flux establishes a steady-state current

$$j_x = \frac{\hbar\mathcal{J}\zeta/2es\Gamma}{L/\sigma + k_BT/\gamma}, \qquad (12)$$

where we took $\gamma_L = \gamma_R = \gamma$ for simplicity. k_BT/γ is the boundary impedance. L/σ is the bulk impedance, scaling linearly with the system size, which dominates in the thermodynamic limit $L \to \infty$. This is similar to the ordinary Ohmic impedance for a conserved electric current. The hedgehog conductivity $\sigma = \rho_0 D/k_BT$ is highly tunable via temperature [37], where ρ_0 and D are the background hedgehog density and the diffusion constant, respectively. In the paramagnetic phase ($T \gtrsim J/k_B$ with J being the exchange energy), let us consider the limiting case where the order parameter varies on the atomic scale. Here, we estimate $\rho_0 \sim 1/a^3$ and $D \sim Ja^2/\hbar$, with a being the lattice spacing. This yields the optimal conductivity $\sigma \sim 1/a\hbar$ in the paramagnetic phase, while $\rho_0 \propto e^{-E_0/k_BT}$ and thus σ is exponentially small in the ordered phase.

The hedgehog current reaching the right terminal exerts a pumping electromotive force on the metal contact [42,44,69], which is determined by invoking the Onsager reciprocity [70]: $\vec{\varepsilon} = \hbar\mathbf{j} \times \vec{\zeta}/2es\Gamma$. This leads to a finite nonlocal drag resistivity (whose sign is opposite to a viscous drag):

$$\varrho \equiv \frac{\varepsilon}{\mathcal{J}} = \frac{(\hbar\zeta/2es\Gamma)^2}{L/\sigma + k_BT/\gamma}, \qquad (13)$$

which is defined as the ratio of the detected voltage (per unit length) along y at the right contact to the injected charge current density at the left contact. In the thermodynamic limit, the bulk impedance dominates and thus the resistivity scales algebraically $\varrho \propto L^{-1}$.

In the ordered phase, hedgehog currents vanish in linear response in the thermodynamic limit, while there can be

transport in finite-size magnets. The magnet behaves like a hedgehog dielectric, which can be polarized by the hedgehog chemical potential provided by the applied electric current in the contact, like a usual dielectric polarized by an electric field. This may be observed directly with coherent diffractive imaging [71,72] or by testing (anti)skyrmion structures on surfaces at two ends [73–75].

Similar to the work on the elastic response of skyrmion crystals [76], one can study the transport feature due to the elasticity of a hedgehog lattice across the hedgehog-lattice melting transition, in the geometry of Fig. 1. To this end, the magnet is replaced by a hedgehog lattice, which should be experimentally accessible [23–25].

Interesting physics emerges when one studies the interplay between electric currents and skyrmion dynamics [46,77,78], such as the skyrmion Hall effect due to the emergent magnetic flux associated with skyrmions. Similarly, we expect hedgehogs to exhibit rich dynamics under electric currents, due to the possible complexity of emergent 3D magnetic field associated with hedgehogs in general.

Discussion.—We note that, though our discussion is based on insulating magnets, it applies equally well to conducting magnets, when the dimension along x is much larger than the other two in Fig. 1, so that we can disregard an Ohmic drag between the side contacts. Our symmetry arguments for the hedgehog injection can also be extended to antiferromagnetic systems, with the Néel order parameter, subject to a careful consideration of the magnetic space group.

There are two interesting open questions we did not address beyond the phenomenological level: the microscopic origin of the spin transfer Eq. (8) and a precise description of confinement-deconfinement transition of hedgehogs. We remark that the proposed nonlocal spin drag experiment in Fig. 1 also serves as a good testing platform of the deconfinement of hedgehogs in the paramagnetic phase.

The advances in coherent diffractive imaging and vector-field tomography have proven promising for direct observations of 3D magnetic textures, as space and time resolutions are under improvement [71,72]. This progress makes it possible for our theoretical concepts and proposals to be experimentally investigated for further understanding and future application of 3D topological spin textures.

Our study broadens the scope of 3D spintronics in at least two aspects: Hedgehogs, as commonly existing topological textures in magnets, are promising to support nonlocal transport in magnets and serve as information carriers. The study of the hedgehog current also offers us a handle to manipulate two-dimensional skyrmion textures, with various potential applications in skyrmionics. Transverse skyrmion textures and their associated free energy can be loaded into a chiral magnet by biasing a

hedgehog flux through it. If the induced skyrmion density can be preserved at lower temperatures, e.g., by the Dzyaloshinskii-Moriya interaction, this would provide a 3D realization of the energy-storage proposal of Ref. [34]. Being able to change the skyrmion number, the hedgehog flow can also be used to flip the polarity of a vortex core, while maintaining the vorticity.

———

*suzy@physics.ucla.edu

[1] S. A. Wolf, D. D. Awschalom, R. A. Buhrman, J. M. Daughton, S. von Molnár, M. L. Roukes, A. Y. Chtchelkanova, and D. M. Treger, Science **294**, 1488 (2001).

[2] I. Žutić, J. Fabian, and S. Das Sarma, Rev. Mod. Phys. **76**, 323 (2004).

[3] V. Baltz, A. Manchon, M. Tsoi, T. Moriyama, T. Ono, and Y. Tserkovnyak, Rev. Mod. Phys. **90**, 015005 (2018).

[4] A. V. Chumak, A. A. Serga, and B. Hillebrands, Nat. Commun. **5**, 4700 (2014).

[5] A. V. Chumak, V. I. Vasyuchka, A. A. Serga, and B. Hillebrands, Nat. Phys. **11**, 453 (2015).

[6] A. Khitun, M. Bao, and K. L. Wang, J. Phys. D **43**, 264005 (2010).

[7] K. Vogt, F. Y. Fradin, J. E. Pearson, T. Sebastian, S. D. Bader, B. Hillebrands, A. Hoffmann, and H. Schultheiss, Nat. Commun. **5**, 3727 (2014).

[8] L. J. Cornelissen, J. Liu, R. A. Duine, J. B. Youssef, and B. J. van Wees, Nat. Phys. **11**, 1022 (2015).

[9] K. Oyanagi, S. Takahashi, L. J. Cornelissen, J. Shan, S. Daimon, T. Kikkawa, G. E. W. Bauer, B. J. van Wees, and E. Saitoh, Nat. Commun. **10**, 4740 (2019).

[10] Y. Tserkovnyak, J. Appl. Phys. **124**, 190901 (2018).

[11] *Topology in Magnetism*, edited by J. Zang, V. Cros, and A. Hoffmann (Springer International Publishing, New York, 2018).

[12] H. Ochoa and Y. Tserkovnyak, Int. J. Mod. Phys. B **33**, 1930005 (2019).

[13] S. K. Kim, S. Takei, and Y. Tserkovnyak, Phys. Rev. B **92**, 220409(R) (2015).

[14] S. C. Chae, N. Lee, Y. Horibe, M. Tanimura, S. Mori, B. Gao, S. Carr, and S.-W. Cheong, Phys. Rev. Lett. **108**, 167603 (2012).

[15] F. P. Chmiel, N. W. Price, R. D. Johnson, A. D. Lamirand, J. Schad, G. van der Laan, D. T. Harris, J. Irwin, M. S. Rzchowski, C. B. Eom, and P. G. Radaelli, Nat. Mater. **17**, 581 (2018).

[16] J. Zou, S. K. Kim, and Y. Tserkovnyak, Phys. Rev. B **99**, 180402(R) (2019).

[17] Y. Tserkovnyak and J. Zou, Phys. Rev. Research **1**, 033071 (2019).

[18] K. Everschor-Sitte, J. Masell, R. M. Reeve, and M. Kläui, J. Appl. Phys. **124**, 240901 (2018).

[19] W. Jiang, P. Upadhyaya, W. Zhang, G. Yu, M. B. Jungfleisch, F. Y. Fradin, J. E. Pearson, Y. Tserkovnyak, K. L.

Wang, O. Heinonen, S. G. E. te Velthuis, and A. Hoffmann, Science **349**, 283 (2015).

[20] H. Ochoa, S. K. Kim, and Y. Tserkovnyak, Phys. Rev. B **94**, 024431 (2016).

[21] X. S. Wang, A. Qaiumzadeh, and A. Brataas, Phys. Rev. Lett. **123**, 147203 (2019).

[22] Y. Liu, W. Hou, X. Han, and J. Zang, Phys. Rev. Lett. **124**, 127204 (2020).

[23] Y. Fujishiro, N. Kanazawa, T. Nakajima, X. Z. Yu, K. Ohishi, Y. Kawamura, K. Kakurai, T. Arima, H. Mitamura, A. Miyake, K. Akiba, M. Tokunaga, A. Matsuo, K. Kindo, T. Koretsune, R. Arita, and Y. Tokura, Nat. Commun. **10**, 1059 (2019).

[24] T. Tanigaki, K. Shibata, N. Kanazawa, X. Yu, Y. Onose, H. S. Park, D. Shindo, and Y. Tokura, Nano Lett. **15**, 5438 (2015).

[25] N. Kanazawa, S. Seki, and Y. Tokura, Adv. Mater. **29**, 1603227 (2017).

[26] P. Nikolić, Phys. Rev. B **101**, 115144 (2020).

[27] X.-X. Zhang, A. S. Mishchenko, G. De Filippis, and N. Nagaosa, Phys. Rev. B **94**, 174428 (2016).

[28] N. Kanazawa, Y. Nii, X. X. Zhang, A. S. Mishchenko, G. De Filippis, F. Kagawa, Y. Iwasa, N. Nagaosa, and Y. Tokura, Nat. Commun. **7**, 11622 (2016).

[29] R. Zarzuela, H. Ochoa, and Y. Tserkovnyak, Phys. Rev. B **100**, 054426 (2019).

[30] D. A. Allwood, G. Xiong, C. C. Faulkner, D. Atkinson, D. Petit, and R. P. Cowburn, Science **309**, 1688 (2005).

[31] A. Fert, V. Cros, and J. Sampaio, Nat. Nanotechnol. **8**, 152 (2013).

[32] S. S. P. Parkin, M. Hayashi, and L. Thomas, Science **320**, 190 (2008).

[33] A. Fert, Rev. Mod. Phys. **80**, 1517 (2008).

[34] Y. Tserkovnyak and J. Xiao, Phys. Rev. Lett. **121**, 127701 (2018).

[35] D. Jones, J. Zou, S. Zhang, and Y. Tserkovnyak, Phys. Rev. B **102**, 140411 (2020).

[36] M. Nakahara, *Geometry, Topology and Physics*, 2nd ed. (CRC Press, Boca Raton, FL, 2003).

[37] See Supplemental Material at http://link.aps.org/supplemental/10.1103/PhysRevLett.125.267201 for (i) proof of the topological conservation law, (ii) topological conservation law of hedgehogs on a quantum lattice, (iii) electric charge distribution for global dynamics, and (iv) hedgehog conductivity from collective variable approach, which cites Ref. [38–40].

[38] M. Stone, Phys. Rev. B **53**, 16573 (1996).

[39] A. Einstein, Ann. Phys. (Berlin) **322**, 549 (1905).

[40] X.-G. Wen, *Quantum Field Theory of Many-body Systems: From the Origin of Sound to an Origin of Light and Electrons* (Oxford University Press, Oxford, 2007).

[41] P. Milde, D. Köhler, J. Seidel, L. M. Eng, A. Bauer, A. Chacon, J. Kindervater, S. Mühlbauer, C. Pfleiderer, S. Buhrandt, C. Schütte, and A. Rosch, Science **340**, 1076 (2013).

[42] G. E. Volovik, J. Phys. C **20** (1987).

[43] N. Nagaosa and Y. Tokura, Phys. Scr. **T146**, 014020 (2012).

[44] C. H. Wong and Y. Tserkovnyak, Phys. Rev. B **80**, 184411 (2009).

[45] G. Tatara, Physica (Amsterdam) **106E**, 208 (2019).

[46] T. Schulz, R. Ritz, A. Bauer, M. Halder, M. Wagner, C. Franz, C. Pfleiderer, K. Everschor, M. Garst, and A. Rosch, Nat. Phys. **8**, 301 (2012).

[47] S. A. Díaz, J. Klinovaja, and D. Loss, Phys. Rev. Lett. **122**, 187203 (2019).

[48] K. A. van Hoogdalem, Y. Tserkovnyak, and D. Loss, Phys. Rev. B **87**, 024402 (2013).

[49] S. Coleman, *Aspects of Symmetry: Selected Erice Lectures* (Cambridge University Press, Cambridge, England, 1988).

[50] A. M. Polyakov, *Gauge Fields and Strings* (CRC Press, Boca Raton, FL, 1987).

[51] H. Brezis, J.-M. Coron, and E. H. Lieb, Commun. Math. Phys. **107**, 649 (1986).

[52] J. B. Kogut, Rev. Mod. Phys. **55**, 775 (1983).

[53] L. P. Kadanoff, Rev. Mod. Phys. **49**, 267 (1977).

[54] L. McLerran, Rev. Mod. Phys. **58**, 1021 (1986).

[55] H. Bohr and H. Nielsen, Nucl. Phys. **B128**, 275 (1977).

[56] W. Cassing and E. L. Bratkovskaya, Phys. Rev. C **78**, 034919 (2008).

[57] A. Peshier and W. Cassing, Phys. Rev. Lett. **94**, 172301 (2005).

[58] H. B. Nielsen and P. Olesen, Nucl. Phys. **B61**, 45 (1973).

[59] Y. Nambu, Phys. Rev. D **10**, 4262 (1974).

[60] G. Hooft, Nucl. Phys. **B79**, 276 (1974).

[61] J. S. Ball and A. Caticha, Phys. Rev. D **37**, 524 (1988).

[62] M. Cardoso, P. Bicudo, and P. D. Sacramento, Ann. Phys. (Amsterdam) **323**, 337 (2008).

[63] Y. Akagi, M. Udagawa, and Y. Motome, Phys. Rev. Lett. **108**, 096401 (2012).

[64] S. Okumura, S. Hayami, Y. Kato, and Y. Motome, Phys. Rev. B **101**, 144416 (2020).

[65] C. Schütte and A. Rosch, Phys. Rev. B **90**, 174432 (2014).

[66] S. Takei and Y. Tserkovnyak, Phys. Rev. Lett. **112**, 227201 (2014).

[67] S. K. Kim, R. Myers, and Y. Tserkovnyak, Phys. Rev. Lett. **121**, 187203 (2018).

[68] P. Hänggi, P. Talkner, and M. Borkovec, Rev. Mod. Phys. **62**, 251 (1990).

[69] Y. Tserkovnyak and M. Mecklenburg, Phys. Rev. B **77**, 134407 (2008).

[70] L. Onsager, Phys. Rev. **37**, 405 (1931).

[71] C. Donnelly, M. Guizar-Sicairos, V. Scagnoli, S. Gliga, M. Holler, J. Raabe, and L. J. Heyderman, Nature (London) **547**, 328 (2017).

[72] C. Donnelly, S. Finizio, S. Gliga, M. Holler, A. Hrabec, M. Odstrčil, S. Mayr, V. Scagnoli, L. J. Heyderman, M. Guizar-Sicairos, and J. Raabe, Nat. Nanotechnol. **15**, 356 (2020).

[73] N. Romming, C. Hanneken, M. Menzel, J. E. Bickel, B. Wolter, K. von Bergmann, A. Kubetzka, and R. Wiesendanger, Science **341**, 636 (2013).

[74] G. Chen and A. K. Schmid, Adv. Mater. **27**, 5738 (2015).

[75] N. Rougemaille and A. Schmid, Eur. Phys. J. Appl. Phys. **50**, 20101 (2010).

[76] H. Ochoa, S. K. Kim, O. Tchernyshyov, and Y. Tserkovnyak, Phys. Rev. B **96**, 020410(R) (2017).

[77] M. Stier, W. Häusler, T. Posske, G. Gurski, and M. Thorwart, Phys. Rev. Lett. **118**, 267203 (2017).

[78] K. Everschor-Sitte, M. Sitte, T. Valet, A. Abanov, and J. Sinova, New J. Phys. **19**, 092001 (2017).